Self-Compensation in Manganese-Doped Ferromagnetic Semiconductors

Steven C. Erwin and A. G. Petukhov*

Center for Computational Materials Science, Naval Research Laboratory, Washington, D.C. 20375

(Received 12 June 2002; published 6 November 2002)

We present a theory of interstitial Mn in Mn-doped ferromagnetic semiconductors. Using density-functional theory, we show that under the nonequilibrium conditions of growth, interstitial Mn is easily formed near the surface by a simple low-energy adsorption pathway. In GaAs, isolated interstitial Mn is an electron donor, each compensating two substitutional Mn acceptors. Within an impurity-band model, partial compensation *promotes* ferromagnetic order below the metal-insulator transition, with the highest Curie temperature occurring for 0.5 holes per substitutional Mn.

DOI: 10.1103/PhysRevLett.89.227201 PACS numbers: 75.50.Pp, 68.43.–h, 71.55.Eq, 75.10.–b

Ferromagnetism in dilute magnetic semiconductors is generally believed to be mediated by carriers — electrons or holes — originating from the magnetic dopants themselves. For example, an isolated Mn impurity in GaAs can substitute for Ga and contribute one hole, which is weakly bound to its acceptor core [1]. GaAs samples with Mn dopant concentrations in the range 1%–2% are ferromagnetic insulators, while samples in the range 3%–6% are ferromagnetic metals [2]. In the metallic phase, the nominal hole concentration, p, is, in principle, equal to the number of Mn atoms per unit volume. Measured hole concentrations are much smaller, by factors ranging from ~ 3 for MnGaAs [2] to ~ 10 or more for MnGe [3]. In most theories of ferromagnetism in dilute magnetic semiconductors, reduced hole concentrations suppress the Curie temperature [4–6]. The reverse scenario — raising the Curie temperature by increasing the hole concentration — is therefore of great current interest. For current theoretical reviews, see Refs. [5,6].

Recent experiments show a strong correlation between Curie temperature, carrier concentration, and the fraction of Mn found at interstitial sites [7]. In this paper, we address several questions not yet settled by experiment. (1) By what mechanism are interstitials formed, given that their calculated formation energies are considerably higher than substitutionals? (2) What determines the relative abundance of interstitials and substitutionals? (3) Under what (doping) conditions do interstitials act as compensators? (4) What role does compensation play in the ferromagnetism?

To answer these questions, we use density-functional theory (DFT) to establish the following: (i) During the MnGaAs growth, Mn adatoms follow a very simple low-energy pathway to directly form interstitial Mn near the surface. (ii) The deposition of additional As converts some of these interstitials to substitutional sites. (iii) The remaining interstitial Mn atoms act as donors, each compensating two substitutional acceptors. Finally, we show that, within an impurity-band model, ferromagnetism below the metal-insulator transition is most favorable — in the sense of the highest Curie temperature — for 0.5 holes per substitutional Mn.

For MnGaAs grown by molecular-beam epitaxy, recent channeling Rutherford backscattering experiments show that as much as $\sim 15\%$ of the total Mn may be interstitial [7]. An open theoretical question is how interstitial Mn might be formed, under what conditions, and in what concentration. For a system in thermodynamic equilibrium, the concentration of each impurity species is determined by its formation energy. Our calculations (described below) show that the equilibrium concentration of interstitial Mn is negligible. But thermodynamic equilibrium can be achieved only if local metastable configurations can be readily overcome. We find that the energy barriers separating interstitial and substitutional configurations do not satisfy this criterion. Hence, equilibrium thermodynamics is not a reliable guide for studying the formation of interstitial Mn.

To investigate the incorporation of Mn under nonequilibrium conditions, one must identify specific reaction pathways and calculate their energy barriers. At low Mn concentrations, the growth of MnGaAs at low temperatures is governed by the potential-energy surface for individual Mn adatoms adsorbing and diffusing on the GaAs surface. We confine our attention to the GaAs(001) surface, the standard orientation for growing MnGaAs. Under As-rich conditions, the GaAs(001) surface can have several different reconstructions, all of which contain surface As dimers as a common building block. Thus, we studied adsorption on a chemically reasonable model surface consisting of five layers of bulk GaAs plus a dimerized As top layer; the bottom layer was passivated. We calculated total energies and forces using pseudopotentials and the generalized-gradient approximation [8,9]. To identify the lowest energy adsorption site, we placed the Mn adatom at various surface sites in a (2×2) supercell, then relaxed the height of the adatom and the positions of all atoms in the top five layers. By far, the most stable adsorption site was the As-dimer bridge site, i.e., equidistant from the two As atoms in a dimer.

To identify specific adsorption pathways, we calculated the total energy on a grid of Mn positions in a plane normal to the surface and containing the As dimer. The resulting potential-energy surface and several possible

adsorption pathways are shown in Fig. 1. Beginning from a height of several angstroms, Mn adatoms are attracted to the surface and at low kinetic energies will be "funneled" into one of two adsorption channels. The primary channel leads to the As-dimer bridge site. As shown in the inset of Fig. 1, there are two locally stable adsorption positions above the As dimer: a shallow metastable site 2 Å above the surface and a stable site 2 Å *below* the surface and more favorable by 0.8 eV. These two minima are separated by a small barrier of 0.2 eV, associated with the opening of the As dimer, which is easily overcome at normal growth temperatures. (In comparison, Ga adatoms also have two locally stable adsorption sites, in agreement with Ref. [10]. However, for Ga the interstitial position is very unfavorable, and the stable site near the surface layer ultimately leads to completely substitutional incorporation [11].) Isolated Mn adatoms that are steered into this primary channel will generally reach their equilibrium position below the As dimer. This position corresponds to a bulk interstitial site with four neighboring As atoms. With the Mn atom at this position, the As dimer above it remains intact with a slightly strained bond. A secondary adsorption channel leads, with no energy barrier, to the cave site between adjacent dimer rows; upon continued growth of GaAs, this site will also correspond to a bulk interstitial site. Thus, we have identified a set of very low-energy pathways which initially steer isolated Mn adatoms to interstitial sites.

Although the energetics of Mn on clean GaAs leads to incorporation only at interstitial sites, the subsequent deposition of additional GaAs can change this situation and lead to partial substitutional incorporation. To illustrate this, we computed the change in Mn binding energy resulting from an additional half monolayer of Ga or As on the surface. In the presence of either a Ga or As adlayer, the surface As-dimer bond breaks and the metastable Mn site above it then corresponds to a substitutional site in the zinc-blende lattice. The adlayer completes the fourfold coordination of this site and, hence, may change its stability relative to the interstitial site. The change depends on the type of adlayer: For a Ga adlayer, the Mn interstitial site remains 0.8 eV more favorable than the substitutional site, but for an As adlayer this difference is reduced to just 0.1 eV. This reduction reflects the crossover from the case of Mn adatoms on clean GaAs (which favors interstitials) to the thermodynamic limit of isolated Mn in bulk GaAs (which favors substitutionals), and suggests that during the growth Mn will be incorporated at both interstitial and substitutional sites.

The electrical activity of a Mn impurity is determined by its formation energy as a function of its charge state. We used DFT to calculate the formation energies of substitutional and interstitial Mn using supercells containing 54 atoms, with convergence checks using 128 atoms. We fixed the chemical potentials to correspond to the As-rich, Mn-rich conditions normally used in growth. Figure 2 shows the resulting formation energies, as a function of the Fermi level, for charge states that are stable within the GaAs band gap. Substitutional Mn is an acceptor, with stable $1-$ and neutral charge states. The theoretical acceptor ionization energy is 100 meV, in good agreement with the experimental value of 113 meV [1]. Interstitial Mn is a deep donor, with stable $2+$, $1+$, and neutral charge states; its donor levels have not been measured experimentally. For *p*-type material, corresponding to the Fermi level near the valence band edge, each interstitial will compensate two substitutionals, in

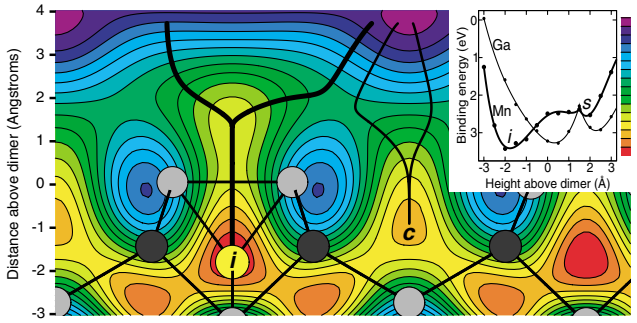

FIG. 1 (color). Potential-energy surface for Mn adsorption on GaAs(001), plotted in a plane normal to the surface and containing the As surface dimer. The minimum energy adsorption site is the subsurface interstitial site labeled *i*; the corresponding surface geometry is shown (light gray for As, dark gray for Ga, yellow for Mn). Typical adsorption pathways funnel Mn adatoms to this interstitial site (heavy curves) or to a cave site, *c* (light curves). Inset: Binding energy of a Mn adatom centered on the As dimer; for comparison, results are also shown for a Ga adatom. When additional As is deposited, the metastable Mn site, *s*, becomes more favorable and leads to partial incorporation of substitutional Mn.

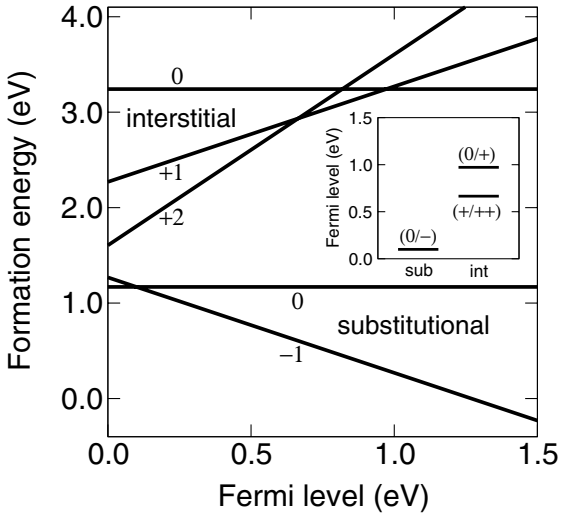

FIG. 2. Formation energies of isolated Mn impurities in GaAs, for different charge states as a function of the Fermi level. Inset: Transition levels (crossing points of the formation energies) between stable charge states of substitutional and interstitial Mn impurities.

agreement with previous calculations [12,13]. The resulting hole concentration is $p = (x - 2y)(4/a^3)$, where x and y are the number of substitutionals and interstitials per Ga site, and a is the GaAs lattice constant.

The consequences of partial compensation for ferromagnetism are different above and below the metal-insulator transition. In the metallic phase, the Mn-induced impurity states broaden and merge with the GaAs valence band. Most current theories therefore consider the carriers as free holes in the valence band. In this picture, the Curie temperature is proportional to $p^{1/3}$, and, hence, compensation can only reduce the Curie temperature. But the role of compensation is less obvious for Mn concentrations between 1% and 2%, where ferromagnetism persists experimentally even though transport data clearly show the samples to be insulating [2]. The nature of this insulating state is not currently understood. If the Coulomb U is larger than the impurity bandwidth, then this state is a Mott-Hubbard insulator and an impurity-band model with localized carriers is an appropriate starting point [14]. Below, we show that, within such a model, the compensation affects the magnetic interactions in a surprising way: The maximum Curie temperature is obtained not for zero compensation, but rather for a partially compensated system with 0.5 holes per substitutional Mn.

We derive this result starting from a Zener double-exchange Hamiltonian for the motion of holes in a narrow impurity band [15],

$$H_{\mathrm{DE}} = \sum_{i\sigma} \epsilon_i a^{\dagger}_{i\sigma} a_{i\sigma} + \sum_{ij\sigma} t_{ij} a^{\dagger}_{i\sigma} a_{j\sigma} - J_H \sum_i \vec{s}_i \cdot \vec{S}_i. \quad (1)$$

The first term describes fluctuations in the on-site impurity levels caused by the random distribution of charged (A^-) and neutral (A^0) Mn acceptors; the second term describes the hopping of holes between Mn spins; and the last term describes the exchange coupling between holes and Mn spins. The energies ϵ_i are distributed within the disorder-broadened bandwidth, W; $a^{\dagger}_{i\sigma}$ and $a_{i\sigma}$ are creation and annihilation operators for holes with spin σ at site i; t_{ij} are hopping integrals; J_H is the exchange coupling constant; $\vec{s}_i$ and $\vec{S}_i$ are the operators for the hole and Mn ($S = 5/2$) spins, respectively.

It is well established that the coupling between the hole and the Mn spin is antiferromagnetic, $J_H < 0$, and that $S|J_H|$ is in the range 100–250 meV [4,16]. This is comparable to, or even larger than, the acceptor ionization energy. Hence, the hole at site i is always antiparallel to the Mn spin, and the Hamiltonian can be reduced to a spinless form with the hopping renormalized to $t_{ij}\cos(\theta_{ij}/2)$, where θ_{ij} is the angle between $\vec{S}_i$ and $\vec{S}_j$.

To second order in the hopping, H_{DE} can be mapped to an effective Heisenberg Hamiltonian describing the interaction between Mn spins,

$$H_{\mathrm{eff}} = \frac{1}{2}\sum_{ij} \frac{|t_{ij}|^2}{\epsilon_i - \epsilon_j}(n_i - n_j)\left(1 + \frac{\vec{S}_j \cdot \vec{S}_j}{S(S+1)}\right), \quad (2)$$

where n_i is the number of holes at site i (thus, $n_i = 0$ and 1 correspond to A^- and A^0 acceptors, respectively). Two features of H_{eff} are noteworthy. First, the effective coupling between spins falls off exponentially with their separation, r_{ij}, because the hopping integrals have the form $t_{ij} = t_0(r_{ij})\exp(-r_{ij}/a_0)$, where $t_0(r) \propto r/a_0$ for hydrogenic wave functions and a_0 is the effective Bohr radius of the Mn acceptor [17]. Second, because of the factor $(n_i - n_j)$, interactions occur only between Mn acceptors in different charge states, that is, between A^0 and A^-. *This implies that ferromagnetism is absent in the limiting cases of no compensation and complete compensation.*

This result can be easily understood within a simple toy model. Consider the Hamiltonian H_{DE} applied to two Mn acceptors that share either zero, one, or two holes. In the case of zero holes (both A^- acceptors), there is no interaction at all. For one hole (A^0 and A^-), the interaction is ferromagnetic, because the hole can lower its kinetic energy via hopping only for aligned spins. For two holes (both A^0), the interaction is always antiferromagnetic and scales as t_{ij}^2/J_H. In the real system, aligning the spins in the absence of compensation drives the Fermi level into the gap between spin-up and spin-down states, making ferromagnetism unfavorable.

To find the Curie temperature of the ferromagnetic phase transition, we first note that mean-field theory is not well justified because of the exponential dependence of the integrals t_{ij} and because of the Mn positional disorder [18–20]. Instead, we represent the system as a percolation network of randomly distributed sites, each occupied by either A^0 or A^-, with interactions only between sites with different charges. In the standard solution to this two-color percolation problem [21], the critical percolation radius, R_c, depends on the solution of the one-color problem and on the maximum eigenvalue of the connectivity matrix for the two-color problem. In our case, this leads to

$$R_c = a\left(\frac{B_c}{(16\pi/3)x\sqrt{q(1-q)}}\right)^{1/3}, \quad (3)$$

where $B_c = 2.7$ is the average number of bonds within the critical radius for the one-color problem [21], and q is the number of holes per substitutional Mn. In general, q must be found from the electroneutrality condition and the energy levels in Fig. 2, but at reasonable temperatures the approximation $q = 1 - 2y/x$ is extremely accurate for $y < x/2$. Note that, due to the factor $\sqrt{q(1-q)}$, the critical radius diverges for both $y = 0$ and $y = x/2$, consistent with our earlier conclusion that ferromagnetism vanishes at these limits.

The Curie temperature is given within percolation theory by

$$k_B T_c = \frac{1}{6} B_c \left\langle \frac{n_i - n_j}{\epsilon_i - \epsilon_j} \right\rangle_{R_c} t_0(R_c)^2 \exp(-2R_c/a_0), \quad (4)$$

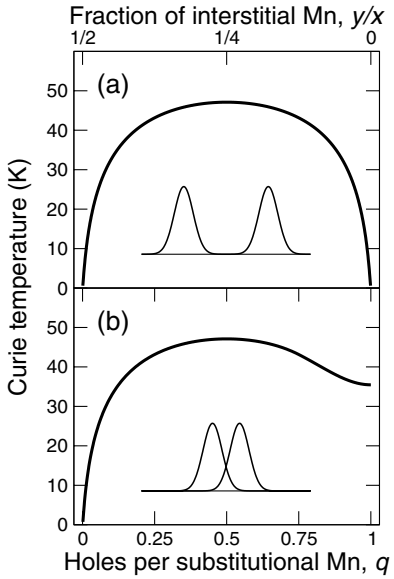

FIG. 3. Dependence of Curie temperature on hole concentration for 1.5% Mn, in two different insulating regimes. (a) Mott-Hubbard insulator, $U > W$. (b) Anderson localization, with the arbitrary choice $U = 0.65W$. Upper and lower Hubbard bands are shown.

where k_B is the Boltzmann constant. The angle brackets denote the most probable value among atoms within the critical radius. We estimate this value using a hydrogenic impurity wave function with effective Bohr radius $a_0 = 7.8$ Å [14], and take the energy separation near the Fermi level to be the Coulomb gap [17,22], given by $|\epsilon_i - \epsilon_j| \simeq e^2/\kappa r_{ij}$, where e is the electron charge, and $\kappa = 10.66$ is the dielectric constant of GaAs [14]. This gives the Curie temperature simply as

$$k_B T_c = \frac{B_c e^2}{108\kappa a_0}\left(\frac{2R_c}{a_0}\right)^3 \exp(-2R_c/a_0). \qquad (5)$$

We show in Fig. 3(a) the dependence of the Curie temperature on the number of holes per substitutional Mn and, equivalently for the case of pure self-compensation, on the fraction of interstitial Mn. The maximum Curie temperature is reached for $q = 0.5$ holes per substitutional Mn, corresponding to $y = x/4$.

The above theory ignores the orbital degeneracy of the impurity band. This simplification is justified if the Coulomb energy, U, of two holes in different orbital states is larger than both the hopping integral and the impurity bandwidth, W. For the case when U is smaller than W, the resulting overlap of the two Hubbard bands will lead to a finite density of states at the Fermi level, even without compensation. For Mn concentrations between 1% and 2%, the materials are nonetheless insulating, suggesting that the states are localized by an Anderson transition induced by strong disorder. In this case, hopping — and thereby also ferromagnetic coupling — can take place not only between A^0 and A^-, but also between A^0 and A^+ acceptors. The percolation radius is still given by Eq. (3), but q now must be replaced by the fraction of neutral acceptors, which must be calculated from the density of states. For a simple triangular density of states, the resulting Curie temperature is shown in Fig. 3(b). One significant new feature arises: Ferromagnetism now persists even without compensation. Otherwise, the main features of the Mott-Hubbard case are obtained here as well, and the maximum Curie temperature is again reached for $q = 0.5$.

This work was supported by the Office of Naval Research, the DARPA SpinS program, and NSF Grant No. DMR-0071823. We thank C. S. Hellberg and I. I. Mazin for helpful discussions.

*Permanent address: Physics Department, South Dakota School of Mines and Technology, Rapid City, SD 57701.

[1] J. Schneider, U. Kaufmann, W. Wilkening, M. Baeumler, and F. Köhl, Phys. Rev. Lett. **59**, 240 (1987).
[2] H. Ohno, J. Magn. Magn. Mater. **200**, 110 (1999).
[3] Y. D. Park, A. Hanbicki, S. C. Erwin, C. S. Hellberg, J. M. Sullivan, J. E. Mattson, T. F. Ambrose, A. Wilson, G. Spanos, and B. T. Jonker, Science **295**, 651 (2001).
[4] T. Dietl, H. Ohno, F. Matsukura, J. Cibert, and D. Ferrand, Science **287**, 1019 (2000).
[5] S. Sanvito, G. Theurich, and N. A. Hill, J. Supercond. **15**, 85 (2002).
[6] J. König, J. Schliemann, T. Jungwirth, and A. H. MacDonald, cond-mat/0111314.
[7] K. Yu, W. Walukiewicz, T. Wojtowicz, and J. Furdyna, Phys. Rev. B **65**, 201303(R) (2002).
[8] G. Kresse and J. Hafner, Phys. Rev. B **47**, 558 (1993).
[9] G. Kresse and J. Fürthmuller, Phys. Rev. B **54**, 11 169 (1996).
[10] A. Kley, P. Ruggerone, and M. Scheffler, Phys. Rev. Lett. **79**, 5278 (1997).
[11] P. Kratzer and M. Scheffler, Phys. Rev. Lett. **88**, 036102 (2002).
[12] Y. H. Chang and C. H. Park, J. Korean Phys. Soc. **39**, 324 (2001).
[13] J. Masek and F. Maca, Phys. Rev. B **65**, 235209 (2002).
[14] M. Berciu and R. N. Bhatt, Phys. Rev. Lett. **87**, 107203 (2001).
[15] Y. A. Izyumov and Y.W. Skryabin, Phys. Usp. **44**, 109 (2001).
[16] F. Matsukura, H. Ohno, A. Shen, and Y. Sugawara, Phys. Rev. B **57**, R2037 (1998).
[17] B. I. Shklovskii and A. L. Efros, *Electronic Properties of Doped Semiconductors* (Springer-Verlag, Berlin, 1984).
[18] I. Y. Korenblit and E. F. Shender, Sov. Phys. Usp. **21**, 832 (1978).
[19] V. I. Litvinov and N. K. Dugaev, Phys. Rev. Lett. **86**, 5593 (2001).
[20] A. Kaminski and S. Das Sarma, Phys. Rev. Lett. **88**, 247202 (2002).
[21] A. S. Ioselevich, Phys. Rev. Lett. **74**, 1411 (1995).
[22] A. L. Efros, Phys. Rev. Lett. **68**, 2208 (1992).